Journal of Thermal Analysis, Vol. 54 (1998) 501-519

TEMPERATURE-MODULATED DIFFERENTIAL SCANNING CALORIMETRY THROUGH HEAT DIFFUSION ANALYSIS

*F. U. Buehler, C. J. Martin and J. C. Seferis**

Polymeric Composites Laboratory, University of Washington, Seattle, WA 98195, USA

Abstract

In the present study, a complete model of thermal diffusion in a TMDSC specimen is presented. The governing equation takes into account thermal conductivity and does not neglect temperature gradients. This model is solved analytically for a specimen of cylindrical geometry with two surfaces following the block temperature and considering the third surface insulated. The full analytical solution consists of a transient and an asymptotic expression. The asymptotic expression is divided into an underlying and a cyclic part to allow comparison with existing models. The present model finds that the phase angle between the temperatures of sample and block are dependent upon the sample material, which has not been predicted by existing models. Moreover, the present model does not require the use of an experimentally determined constant as long as the cell is ideal. It was found that the phase lag between sample and block temperatures could be described by two effective thermal diffusivities, Λ' and Λ'', instead of complex heat capacities c_p' and c_p''. These heat capacity parameters were viewed as mathematical artifacts arising from the use of an over-simplified governing equation that does not take into account thermal conductivity and thermal gradients within the specimen.

Keywords: complex heat capacity, heat transfer, phase lag, TMDSC

Introduction

Temperature Modulated Differential Scanning Calorimetry, or TMDSC, MTDSC, is a rather new technique that was conceived in the early 90's by Reading and co-workers and commercialized by TA Instruments [1–3]. The advantage of TMDSC compared to conventional DSC is that the temperature signal can be modulated as a sinusoidal wave, and be superimposed over the traditional heating rate. This technique offers the possibility of deconvoluting the signal into an in-phase and an out-of-phase response, which can be used to calculate heat flows or heat capacities [1, 2, 4].

* Author to whom all correspondence should be addressed.

1418–2874/98/ $ 5.00

Akadémiai Kiadó, Budapest
Kluwer Academic Publishers, Dordrecht

In 1985, Birge and Nagel performed an experiment with a sinusoidal heat flux applied to a sample [5]. This technique is also known as AC calorimetry [6]. Birge and Nagel reported that the product of $c_p k$ was measured, where c_p is the specific heat capacity of the sample and k is its thermal conductivity. This product was found to have a real and an imaginary component. However, the authors estimated the contribution of k to be very small and therefore considered only that of c_p and deconvoluted the product of c_p and k into $c_p' k$ and $c_p'' k$. Reading *et al.* applied an oscillatory condition to a traditional heat flux DSC and through a discrete Fourier transformation the resulting signal was separated into total, reversing, and non-reversing heat flows [3]. This method was commercialized as TMDSC and reinforced the idea of a complex heat capacity. Many authors followed on this concept, including Gill and Schawe [7–9]. Furthermore, Schawe proposed a frequency dependent c_p, which has been observed under certain conditions by Birge and Nagel [5].

The existence of a complex heat capacity has troubled many scientists over the past years. Heat capacity is a scalar that is thermodynamically defined as the derivative of enthalpy with respect to temperature at either constant pressure or volume. Some authors have tried to justify the existence of a complex heat capacity from a thermodynamical viewpoint based on entropy, while others suggest c_p'' to be linked to dissipative phenomena [5, 8–11]. However, no entropic origin can be attributed to c_p'' using reversible thermodynamics as the derivative of entropy with respect to temperature at constant pressure is equal to heat capacity over temperature, $(\partial S/\partial T)_p = C_p/T$ [12]. Therefore if entropy does change dependent upon c_p, it does not contribute to a loss heat capacity within the limit of application of reversible thermodynamics. Other authors proposed to use irreversible thermodynamics to explain the origin of c_p'' [13]. However, as noted by Höhne, irreversible thermodynamics is a rather complicated theory which is not yet fully developed [11]. Basically, there is no well-founded physical or thermodynamical interpretation of c_p''. Moreover, heat capacity is a bulk property of the material and is therefore isotropic, very much like density ρ. Heat capacity gradients, as well as density gradients, can exist in heterogeneous materials, but not in homogeneous matter c_p and ρ are not tensors, unlike the thermal conductivity k. The thermal conductivity k can be anisotropic, and is found to be in many materials like carbon fibers. k can be expressed as a tensor, and its anisotropic properties make it a very likely candidate for a complex expression: $k^* = k' + ik''$ [14, 15]. The thermal diffusivity α, which is defined as $k/\rho c_p$, should therefore have a complex part as well, but the c_p'' utilized by many authors might very well be an artifact due to a simplistic mathematical model of the TMDSC.

Numerous mathematical models for the computation of the heat capacity have been published since the commercialization of the TMDSC in the early 1990's. Most of these models consider the sample temperature to be uniform throughout the sample at any time, and begin by equating the heat accumulation

term to Newton's law of cooling [1, 2, 8, 16]. This approach would be acceptable if the average temperature of the sample was measured. However, in the TMDSC instrument, the thermocouples are located at the center bottom of the specimens and therefore measure the local temperature at this point, which is different from the average temperature of the specimen. Although this assumption reduces the governing equation to a single variable (time), it neglects the contribution of thermal conductivity. Foreman *et al.* used TMDSC to determine the thermal conductivity k, and found values that agreed within 3% of the literature values [17]. This clearly showed the importance of k in the TMDSC. Foreman *et al.* proposed a one dimensional model to compute k. However, their work did not provide a rigorous mathematical description and does not explain how thermal gradients within the specimen were accounted for [17]. Lacey and co-workers proposed several mathematical descriptions of heat transfer in the TMDSC cell [18]. The case of one-dimensional as well as three-dimensional models were discussed, one of which accounted for the thermal conductivity k. However, the thermal conductivity was lumped into a calibration factor, and the cylindrical shape of the specimen was not taken into account along with possible different temperature gradients [18]. The problem of the temperature gradients was addressed by Melling *et al.* as early as 1969 for the case of DTA (Differential Thermal Analysis) [19]. Although DTA differs from TMDSC by the absence of modulation and does not quantitatively measure heat flow into and out of the sample, the set-up and the governing equation of heat transfer are similar – only boundary conditions differ. The solution of Melling *et al.* accounted for temperature gradients but only in the radial direction [19]. More recently, Schenker and Stäger investigated the heat transfer under TMDSC conditions, but considered axial heat diffusion only [20].

Accordingly, there is a need for a mathematical model of TMDSC that takes into account both the thermal conductivity and the temperature gradients within the specimens. In the present paper, the analytical solution of the temperature profile within the sample will be derived. Next the effect of the thermal diffusivity on the temperature distribution and phase lag will be investigated. To understand the origin of the out-of-phase response, the results will then be compared to the models which only consider sample heat capacity. It will be shown that an out-of-phase response can be predicted by incorporation of thermal conductivity without the introduction of a complex heat capacity.

Mathematical model

The three-dimensional heat flow model of the specimen shown in Fig. 1 is considered. The DSC pan is assumed to be a right circular cylinder of radius R with parallel end faces. The height of the specimen is L. The specimen symmetry implies a temperature profile that does not depend on the angle Ω, therefore T is

considered to be a function of the axial position z, the radial position r, and the time t. To determine the temperature $T-T(r,z,t)$, the heat diffusion equation:

$$\frac{\partial T}{\partial t} = \alpha \nabla^2 T \tag{1}$$

is expressed in terms of α, the thermal diffusivity of the specimen. Expressing the Laplacian in cylindrical coordinates yields:

$$\frac{\partial T}{\partial t} = \alpha \left[\frac{1}{r} \frac{\partial}{\partial r} \left(r \frac{\partial T}{\partial r} \right) + \frac{\partial^2 T}{\partial z^2} \right] \tag{2}$$

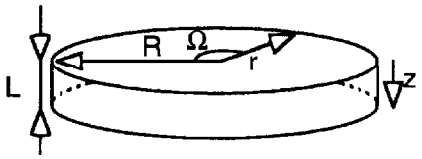

Fig. 1 The DSC pan considered to be a cylinder of radius R and length L. Cylindrical coordinates are used to solve the heat diffusion equation

Boundary conditions

The entire specimen is initially at temperature T_o. The top face and side face of the specimen are presumed to follow the block temperature T_b. The heat flow through the bottom face is considered to be zero. It can be noted that a full model of heat transfer in TMDSC of course would account for heat transfer through the support disk and lower surface of the sample and reference. However, the boundary conditions between the specimen and disk is complex and of the third kind. This would involve solving the heat diffusion equation for the sample, reference, and support disk simultaneously with the matched boundary conditions and is beyond the scope of this paper. Therefore, for the sake of simplicity, it was assumed that the sample is heated from the side and top surfaces and that there was no heat transfer through the bottom surface. Mathematically this gives:

Specimen temperature equals to T_o initially

$$T(r,z,0) = T_o \tag{3}$$

Side surface temperature equals to that of the furnace, T_b

$$T(R,z,t) = T_b \tag{4}$$

Top surface temperature equals to that of the furnace, T_b

$$T(r,0,t) = T_b \tag{5}$$

No heat flux at the bottom surface

$$-k\frac{\partial T}{\partial z}(r,L,t) = 0 \tag{6}$$

Symmetry condition at the center of the specimen

$$\frac{\partial T}{\partial r}(0,z,t) = 0 \tag{7}$$

where the furnace (block) temperature is:

$$T_b = T_{bo} + bt + A\sin(\omega t) \tag{8}$$

In Eq. (8) b is the temperature ramp and A is the amplitude of the modulation. The pulsation ω is equal to 2π over the period of modulation.

Non-dimensionalization

The following change of variables are applied to non-dimensionalize the problem as well as make the inhomogeneous boundary conditions homogenous:

$$\theta = \frac{T - T_b}{T_o} \tag{9}$$

$$x = \frac{r}{R} \tag{10}$$

$$\zeta = \frac{z}{L} \tag{11}$$

$$\tau = \frac{\alpha t}{R^2} \tag{12}$$

The governing equation, Eq. (2), then becomes:

$$\frac{\partial \theta}{\partial \tau} = \left[\frac{1}{x}\frac{\partial}{\partial x}\left(x\frac{\partial \theta}{\partial x}\right)\right] + \left[\frac{R^2}{L^2}\frac{\partial^2 \theta}{\partial \zeta^2}\right] - \left[\frac{bR^2}{\alpha T_o} + \frac{A\omega R^2}{\alpha T_o}\cos\left(\frac{\omega R^2}{\alpha}\tau\right)\right] \tag{13}$$

The initial condition, Eq. (3), becomes:

$$\theta(x,\zeta,0) = 1 - \frac{T_{bo}}{T_o} \tag{14}$$

The boundary conditions, Eqs (4)–(7), become:

$$\theta(1,\zeta,\tau) = 0 \tag{15}$$

$$\theta(x,0,\tau) = 0 \tag{16}$$

$$\frac{\partial\theta}{\partial\zeta}(x,1,\tau) = 0 \tag{17}$$

$$\frac{\partial\theta}{\partial x}(0,\zeta,\tau) = 0 \tag{18}$$

Solution to the heat diffusion equation

The governing equation, Eq. (13), has now one extra term on the right-hand side. This term can be thought of as a source term S and will be treated as such by Green's theorem, viz:

$$S = -\left[\frac{bR^2}{\alpha T_0} + \frac{A\omega R^2}{\alpha T_0}\cos\left(\frac{\omega R^2}{\alpha}\tau\right)\right] \tag{19}$$

First the homogeneous problem, with no source term, is solved. A product solution of the form $\theta(x,\zeta,\tau)=X(x)Z(\zeta)Y(\tau)$ is proposed. This expression is placed in the governing Eq. (13), with S=0, to yield:

$$\frac{1}{Y}\frac{dY}{d\tau} = \left[\frac{1}{xX}\frac{d}{dx}\left(x\frac{dX}{dx}\right)\right] + \frac{R^2}{L^2}\left[\frac{1}{Z}\frac{d^2Z}{d\zeta^2}\right] \tag{20}$$

The boundary conditions (15)–(18) become:

$$X(1) = 0 \tag{21}$$

$$Z(0) = 0 \tag{22}$$

$$\frac{\partial Z}{\partial z}(1) = 0 \tag{23}$$

$$\frac{\partial X}{\partial x}(0) = 0 \tag{24}$$

The first term on the right-hand side of Eq. (20) can be equaled to $-\lambda^2$, the last term in brackets can be equaled to $-\mu^2$, and the total expression can be equaled to $-\kappa^2$. This yields:

$$\frac{1}{Y}\frac{dX}{d\tau} = -\kappa^2 = -\left(\lambda^2 + \frac{R^2}{L^2}\mu^2\right) \tag{25}$$

$$\left[\frac{1}{xX}\frac{\mathrm{d}}{\mathrm{d}x}\left(x\frac{\mathrm{d}X}{\mathrm{d}x}\right)\right]=-\lambda^2 \tag{26}$$

$$\left[\frac{1}{Z}\frac{\mathrm{d}^2Z}{\mathrm{d}\zeta^2}\right]=-\mu^2 \tag{27}$$

Equations (26) and (27), along with boundary conditions (21)–(24), are Sturm-Liouville problems [21]. The characteristic solutions (eigenfunctions) to the Sturm-Liouville problems correspond to an infinite set of characteristic numbers (eigenvalues) [21].

The solutions to Eqs (25)–(27) are found to be:

$$Y(\tau)=A\mathrm{e}^{-\kappa^2\tau} \tag{28}$$

$$X(x)=BJ_0(\lambda x)+CY_0(\lambda x) \tag{29}$$

$$Z(\zeta)=D\sin(\mu\zeta)+E\cos(\mu\zeta) \tag{30}$$

The boundary conditions (22) and (24) imply that E=0 and C=0, respectively. Boundary conditions (21) and (23) give the following eigenvalues:

$$\lambda_n\text{'s satisfy the transcendental equation: } J_0(\lambda_n)=0 \tag{31}$$

$$\mu_p=(2p-1)\frac{\pi}{2}\text{ where } p \text{ is an integer} \tag{32}$$

The solution that was found for $Y(\tau)$ satisfies the problem without source term. However, it has to be rejected for a non-zero source term and the following expression for θ is postulated:

$$\theta(x,\zeta,\tau)=\sum_{n=1}^{\infty}\sum_{p=1}^{\infty}A_{n,p}(\tau)X_n(x)Z_p(\zeta) \tag{33}$$

and now $A_{n,p}(\tau)$ has to be determined. This is done by applying Green's theorem. The following Green's function is defined:

$$G(\tau-\tau';x,x',\zeta,\zeta')=\sum_{n=1}^{\infty}\left(\sum_{p=1}^{\infty}\left[\mathrm{e}^{-\kappa_{n,p}^2(\tau-\tau')}\frac{X_n(x)X_n(x')}{\|X_n\|^2}\frac{Z_p(\zeta)Z_p(\zeta')}{\|Z_p\|^2}\right]\right) \tag{34}$$

where $\|X_n\|^2$ and $\|Z_p\|^2$ are the norms of the eigenfunctions X_n and Z_p.

Applying Green's theorem yields:

$$\theta(x,\zeta,\tau) = \int_0^1\int_0^1 \left(1 - \frac{T_{bo}}{T_o}\right) x' G(\tau\ 0;x,x',\zeta,\zeta')\mathrm{d}x'\mathrm{d}\zeta' + \int_0^\tau\int_0^1\int_0^1 Sx' G(\tau-\tau';x,x',\zeta,\zeta')\mathrm{d}x'\mathrm{d}\zeta'\mathrm{d}\tau' \quad (35)$$

where S is the source term defined in Eq. (19).

The temperature profile resulting from Eq. (35) is:

Although complex the above expression provides for a complete description of a temperature profile response in a typical TMDSC experiment.

$$\theta(x,\zeta,\tau) = \sum_{n=1}^{\infty}\left(\sum_{p=1}^{\infty}\left\{\frac{4}{\mu_p\lambda_n J_1(\lambda_n)}\left[e^{-\kappa_{n,p}^2\tau}\left(1-\frac{T_{bo}}{T_o}+\frac{bR^2}{\alpha T_o\kappa_{n,p}^2}+\frac{A\omega R^2\kappa_{n,p}^2}{\alpha T_o\left(\kappa_{n,p}^4+\frac{R^4\omega^2}{\alpha^2}\right)}\right)-\cdots\right.\right.\right.$$

$$\left.\left.\left.\cdots-\frac{bR^2}{\alpha T_o\kappa_{n,p}^2}-\cdots\right.\right.\right. \quad (36)$$

$$\left.\left.\left.\cdots-\frac{A\omega R^2}{\alpha T_o\left(\kappa_{n,p}^4+\frac{R^4\omega^2}{\alpha^2}\right)}\left(\kappa_{n,p}^2\cos\left(\frac{R^2\omega\tau}{\alpha}\right)+\frac{\omega R^2}{\alpha}\sin\left(\frac{R^2\omega\tau}{\alpha}\right)\right)\right]J_0(\lambda_n x)\sin(\mu_p\zeta)\right\}\right)$$

Application to TMDSC

In the TMDSC apparatus, the temperature recorded by the thermocouple is that of the center bottom surface, which means that it is recorded at x=0 and ζ=1. The non-dimensional variables are replaced by the original variables, the transient terms are dropped for large times (asymptotic solution), x is set to zero, and ζ is set to 1 to yield:

$$T(0,L,t) = \sum_{n=1}^{\infty}\sum_{p=1}^{\infty}\frac{4}{\mu_p\lambda_n J_1(\lambda_n)} \quad (37)$$

$$\left[-\frac{bR^2}{\alpha\kappa_{n,p}^2}-\frac{A\omega R^2}{\alpha\left(\kappa_{n,p}^4+\frac{R^4\omega^2}{\alpha^2}\right)}\left(\kappa_{n,p}^2\cos(\omega t)+\frac{\omega R^2}{\alpha}\sin(\omega t)\right)\right]+T_b$$

Equation (37) applies to both the sample and the reference it can be rewritten under the form:

$$T_i(0,L,t) = bR^2\frac{1}{\alpha_i}\sigma - A\omega R^2\frac{1}{\Lambda_i'}\sin(\omega t) - A\omega R^2\frac{1}{\Lambda_i''}\cos(\omega t) + T_b \tag{38}$$

where i is either r (for the reference) or s (for the sample).

The summation σ and the Λ's are defined as:

$$\sigma = \sum_{n=1}^{\infty}\sum_{p=1}^{\infty} -\frac{4}{\mu_p\lambda_n J_1(\lambda_n)\kappa_{n,p}^2} \tag{39}$$

$$\frac{1}{\Lambda_i'} = \sum_{n=1}^{\infty}\sum_{p=1}^{\infty}\frac{4}{\mu_p\lambda_n J_1(\lambda_n)}\left[\frac{\omega R^2}{(\kappa_{n,p}^4\alpha_i^2 + \omega^2 R^4)}\right] \tag{40}$$

$$\frac{1}{\Lambda_i''} = \sum_{n=1}^{\infty}\sum_{p=1}^{\infty}\frac{4\kappa_{n,p}^2}{\mu_p\lambda_n J_1(\lambda_n)}\left[\frac{\alpha_i}{(\kappa_{n,p}^4\alpha_i^2 + \omega^2 R^4)}\right] \tag{41}$$

Defining the in-phase and out-of-phase magnitude M_i' and M_i'' gives:

$$M_i' = A - A\omega R^2\frac{1}{\Lambda_i'} \tag{42}$$

$$M_i'' = A\omega R^2\frac{1}{\Lambda_i''} \tag{43}$$

and

$$T_i(0,L,t) = bR^2\frac{1}{\alpha_i}\sigma + T_{bo} + bt + M_i'\sin(\omega t) - M_i''\cos(\omega t) \tag{44}$$

A phase lag φ between the temperature oscillation of the block and specimen can be found by rearranging Eq. (44) into a sine form:

$$T_i = \left(bR^2\sigma\frac{1}{\alpha_i} + T_{bo} + bt\right) + M_i^*\sin(\omega t + \varphi_i) \tag{45}$$

where:

$$M_i^* = \sqrt{M_i'^2 + M_i''^2} \tag{46}$$

$$\tan\varphi_i = \left(-\frac{M_i''}{M_i'}\right) \tag{47}$$

It can be seen from Eq. (47) that φ_i is a negative quantity. This indicates that the specimen temperature lags behind that of the block throughout the experiment.

The temperature difference ΔT between the reference and the sample is then:

$$\Delta T = T_r - T_s = bR^2\left(\frac{1}{\alpha_r} - \frac{1}{\alpha_s}\right)\sigma - \tag{48}$$

$$- A\omega R^2\left(\frac{1}{\Lambda'_r} - \frac{1}{\Lambda'_s}\right)\sin(\omega t) - A\omega R^2\left(\frac{1}{\Delta''_r} - \frac{1}{\Lambda''_s}\right)\cos(\omega t)$$

To be consistent with the definitions proposed by Lacey *et al.*, the temperature difference ΔT is split into an underlying part $\bar{\Delta}T$ and a cyclic part $\tilde{\Delta}T$ [18]. The underlying term arises from the traditional DSC temperature ramp, whereas the cyclic term arises from the TMDSC modulation itself.

$$\bar{\Delta}T = bR^2\left(\frac{1}{\alpha_r} - \frac{1}{\alpha_s}\right)\sigma \tag{49}$$

$$\tilde{\Delta}T = A\omega R^2\sqrt{\left(\frac{1}{\Lambda'_r} - \frac{1}{\Lambda'_s}\right)^2 + \left(\frac{1}{\Lambda''_r} - \frac{1}{\Lambda''_s}\right)^2}\sin(\omega t + \Psi) \tag{50}$$

where

$$\tan\Psi = \frac{\frac{1}{\Lambda''_r} - \frac{1}{\Lambda''_s}}{\frac{1}{\Lambda'_r} - \frac{1}{\Lambda'_s}} \tag{51}$$

At this point it is seen that the Λ definitions, Eqs (40) and (41), allow the cyclic part to be expressed in a form analogous to that of the underlying part. Furthermore, an inphase and an out-of-phase component have been defined for the cyclic part under a form which enables a complex (imaginary) description of the problem. The above formulation allows for a description of the problem in terms of material and experimental parameters.

Results and discussion

A numerical simulation of the temperature evolution at the center bottom of the sample was undertaken. It was done with the use of the software Matlab® 4.2c.1 for Windows by The MathWorks, Inc. The parameters used throughout this paper are displayed in Table 1. Oscillation amplitude and period were chosen according to the recommended parameters for the TA Instrument 2920 TMDSC and are typical of standard TMDSC operation. The eigenvalues λ_n's were obtained from reference [22] and the simulation was run in double precision with 20 eigenvalues for λ_n and 20 eigenvalues for μ_p. The thermal diffusivity α_s of the sample was allowed to vary from α_r down to four orders of magnitude below α_r, α_r being the thermal diffusivity of the reference pan.

Table 1 Parameters used for the numerical simulation with typical values [23]

Parameter	Symbol	Value	Unit
Modulation amplitude	A	1	K
Radius of the specimen	R	0.0033	m
Height of specimen	L	0.00074	m
Initial temperature of the sample	T_0	323	K
Isothermal experiment	b	0	$K\ s^{-1}$
Aluminium pan	α_r	$9.71 \cdot 10^{-5}$	$m^2\ s^{-1}$
Modulation period of 60 s	ω	$2\pi/60$	$rad\ s^{-1}$

Figure 2 shows the temperature evolution of the sample, reference, and block as it should be measured by the TMDSC thermocouples over one modulation period after sufficient time was elapsed to remove the transient effects, provided that the pans are identical and the cell symmetric. The sample material in Fig. 2 is polyethylene terephthalate (PET). This material was chosen because it does not exhibit any first order or second order transitions in the temperature range of interest, which makes it an ideal candidate for this study. Also PET curves are available in the literature, which is precious for model comparison [7, 8]. It was found in Fig. 2 that the reference and block temperatures were essentially indistinguishable. The high thermal diffusivity of the reference pan material (aluminum in the present case) does not allow any lag to build up. It can also be seen that the PET sample exhibits a lower temperature amplitude than the block. This lower amplitude is due to the lower thermal diffusivity of PET. The thermal diffusivity of PET is about 1/1000 that of aluminum, hence the slower heat transfer. This is confirmed by the phase lag: the PET temperature evolution on Fig. 2 is

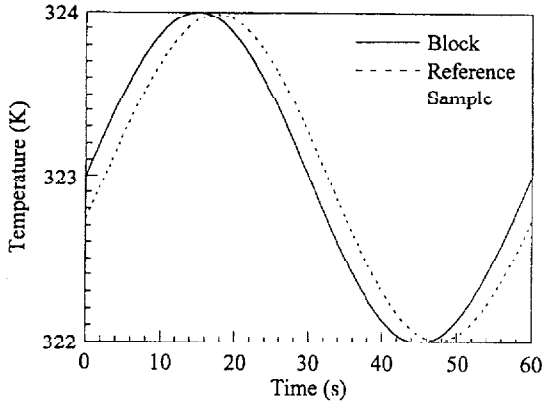

Fig. 2 Temperature evolution of the block, sample, and reference over a period of modulation. Parameters are that mentioned in the Table 1 with α_s of PET ($0.93 \cdot 10^{-7}\ m^2\ s^{-1}$)

lagging behind that of the block and that of the reference by 3.16 s or 19°. This clearly demonstrates the importance of thermal diffusivity in the sample response to temperature modulation.

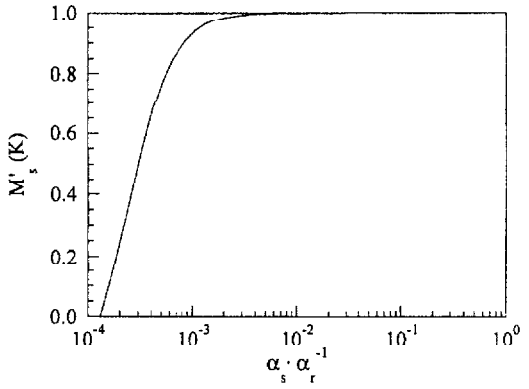

Fig. 3 Dependence of the sample in-phase temperature magnitude, M_s', *vs.* the ratio of the sample and reference thermal diffusivities

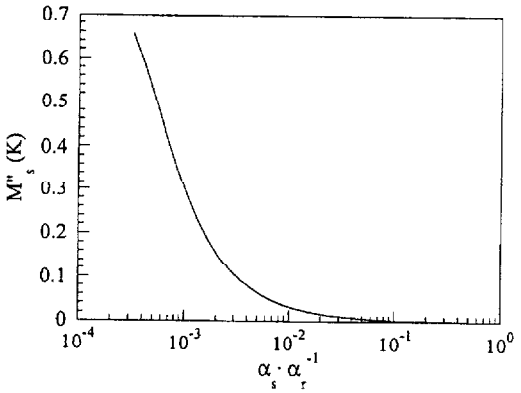

Fig. 4 Dependence of the sample out-of-phase temperature magnitude, M_s'', *vs.* the ratio of the sample and reference thermal diffusivities

To further investigate the effect of thermal diffusivity, the in-phase and out-of-phase components of the sample temperature as well as the phase angle are plotted against the ratio of thermal diffusivities in Figs 3–5. This means that a phase lag can be predicted independent of the cell calibration, as long as the cell is ideal (i.e. without thermal resistance between the cell and sensor and in the absence of cell asymmetry). When $\alpha_s=\alpha_r$, the sample is expected to behave exactly like the reference and this is observed in Figs 3–5: the in-phase component of the sample temperature, M_s', is equal to one (the modulation amplitude), M_s'' (the out-of-phase component of the sample temperature) is equal to zero, and the phase angle φ_s between the temperature signal and the block temperature is insig-

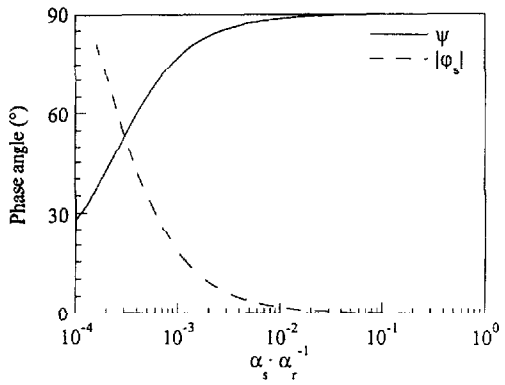

Fig. 5 Dependence of the sample phase angle φ_s and the phase angle ψ *vs.* the ratio of the sample and reference thermal diffusivities

nificant. As α_s decreases, the heat transfer is not as efficient, and this means a decrease in M_s', an increase in M_s'', and a larger phase lag φ, as seen on Figs 3–5. The in-phase sample temperature amplitude, M_s' is found to remain constant until α_s is two orders of magnitude lower than α_r. Below this value, the drop in M_s' is very appreciable. The out-of-phase component of the sample temperature, M_s'', is found to be negligible until α_s drops to about one order of magnitude blow α_r, as seen on Fig. 4. This means that for substances with α_s lower than $\alpha_r/10$, the out-of-phase component starts to take importance and that the phase lag should become appreciable. The phase lag, shown in Fig. 5, becomes appreciable once the thermal diffusivity of the sample is 10 times or more lower than that of the aluminum reference. As shown in Table 2, most polymers have α_s between two and three orders of magnitude below α_r, therefore they fall in the area where the phase angle and the temperature amplitudes of the sample become significantly different from those of the block.

Note however that for very small values of α_s, the sensitivity of TMDSC could be impaired because the transient terms might become important on the time scale of the experiment. A decrease of α_s by an order of magnitude means a time 10 times as long before the transient terms can be neglected. This might be of importance for substances like asphalt or wood that have an extremely low thermal diffusivity, as can be seen in Table 2.

Once the transient terms have vanished at sufficiently long times, the effect of thermal diffusivity on the asymptotic solution can be studied. It is, however, not easy to interpret, especially in the cyclic part of the temperature difference between the reference and the sample. As seen in Eq. (47), the underlying part is an explicit function of α_s and α_r, whereas the cyclic part depends on some complex expression of α_s and Λ' and Λ''. Λ' and Λ'' are in units of $m^2\,s^{-1}$, and can be thought of as the in-phase and the out-of-phase effective thermal diffusivities. Figure 6 shows how the effective thermal diffusivities depend on the α_s/α_r ratio. The in-phase effective thermal diffusivity, Λ', is found to drop sharply as α_s goes

Table 2 Thermal diffusivity α_s of selected non-metallic substances [23–26]

Material	Thermal diffusivity $\cdot 10^6$/ $m^2\ s^{-1}$	α_s/α_r ($\alpha_r=\alpha_{aluminium}=9.71\cdot10^{-5}\ m^2\ s^{-1}$)
Asphalt	0.032	$3.30\cdot10^{-4}$
Poly(isoprene)	0.077	$7.93\cdot10^{-4}$
Yellow pine	0.084	$8.65\cdot10^{-4}$
Poy(ethylene terephthalate)	0.093	$9.58\cdot10^{-4}$
Fir	0.097	$9.99\cdot10^{-4}$
Poly(methyl methacrylate)	0.113	$1.16\cdot10^{-3}$
Oak	0.131	$1.35\cdot10^{-3}$
Cork	0.181	$1.86\cdot10^{-3}$
Poy(vinyl chloride)	0.346	$3.56\cdot10^{-3}$
Urethane foam	0.355	$3.66\cdot10^{-3}$
Cellular glass	0.400	$4.12\cdot10^{-3}$
Extruded poly(styrene)	0.406	$4.18\cdot10^{-3}$
Glass fiber	0.431	$4.44\cdot10^{-3}$
Cement mortar	0.496	$5.11\cdot10^{-3}$
Bakelite	0.719	$7.40\cdot10^{-3}$
Pyrex	0.754	$7.77\cdot10^{-3}$
Ice	1.002	$1.03\cdot10^{-2}$
Vermiculite	1.018	$1.05\cdot10^{-2}$
Granite	1.369	$1.41\cdot10^{-2}$
Polystyrene beads	2.066	$2.13\cdot10^{-2}$
Sapphire	8.300	$8.55\cdot10^{-2}$

from α_r to one tenth of α_r. When α_s reaches about one tenth of α_r, the value of Λ' is extremely small. The out-of-phase effective thermal diffusivity, Λ'', exhibits similar behaviour, but the initial drop is not as sharp and Λ'' reaches low values only when α_s is about 100 times smaller than α_r. Interestingly, when α_s is close to α_r, Λ_s' is three to four orders of magnitude greater than Λ_s''. For values of α_s corresponding to that of polymers shown in Table 2, Λ_s' and Λ_s'' are approximately of the same order of magnitude, indicating that an appreciable phase lag will be observed. Λ' and Λ'' are the two parameters that dictate the behaviour of the specimen and not c_p' and c_p'', as was implied by the many simplified models. The controversial complex heat capacity model can be compared to the model proposed in this paper.

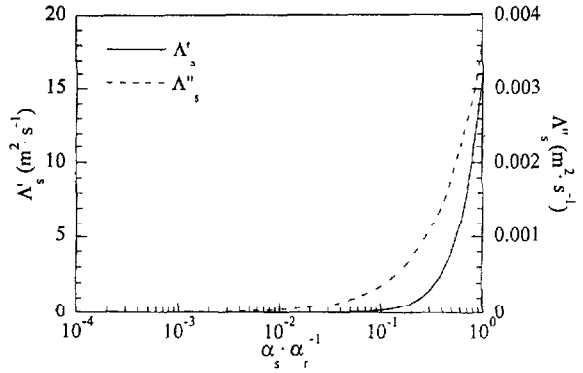

Fig. 6 Value of the sample in-phase and out-of-phase effective thermal diffusivity, Λ'_s and Λ''_s, as a function of the ratio of the sample and reference thermal diffusivities

Table 3 shows the parameters of both models for PET at 50°C. Aubuchon and Gill reported a value of zero for c''_p [7], which was not anticipated by the present model since Λ''_s was estimated as $3.65 \cdot 10^{-6}$ m^2 s^{-1}. This nil c''_p is due to the phase calibration method used by Aubuchon and Gill [7]. They zeroed the phase angle to accommodate for the so-called instrumental phase lag. The actual phase angle that they observed before calibration was 21°, which is 2 degrees higher than the value predicted by the proposed model. This difference can be partially but not completely attributed to cell asymmetry. It should be noted that equating the phase angle to zero is not correct because then the sample contribution is eliminated. The phase calibration should compensate for the instrument non-ideality and leave the sample contribution untouched. In Aubuchon and Gill, it was seen that the values obtained for c'_p and c''_p were dependent upon this phase angle correction, which means that c'_p and c''_p are set on an arbitrary scale by the calibration and that their value has no physical significance. Therefore, the heat capacities c'_p and c''_p are merely mathematical artifacts that appear due to the use of an inadequate model that neglects thermal conductivity and thermal gradients within the sample.

Table 3 Model parameters for PET at 50°C, A=1 K, p=60 s

From Ref. [7]	Proposed model
$c'_p = 1.6$ J g^{-1} K^{-1}	$\Lambda'_s = 1.56 \cdot 10^{-5}$ m^2 s^{-1}
$c''_p = 0$ J g^{-1} K^{-1}	$\Lambda''_s = 3.65 \cdot 10^{-6}$ m^2 s^{-1}
$\varphi - 0°$ after calibration	$\varphi = 19°$
$\varphi = 21°$ before calibration	

The model developed here takes into account thermal conductivity and the thermal gradients in the specimen. It also enables the prediction of the TMDSC temperature profiles without the introduction of mathematical quantities of uncertain physical or thermodynamical significance.

Collectively, we expect that this analysis has provided an interesting contribution to the TMDSC technique so that its results can be analyzed in similar manner to other oscillatory type experiments like dynamic mechanical and dielectric analysis (DMA, DEA).

Conclusions

A rigorous derivation of the heat transfer problem in a cylindrical specimen under TMDSC condition was presented. The mathematical model considered the TMDSC pan to be of cylindrical shape with the side and top surfaces following the temperature of the block. The surface on which the specimen rests was assumed insulated. The three dimensional heat diffusion equation, taking into account thermal conductivity, was solved analytically by using the product method and Green's theorem after appropriate non-dimensionalization. The solution was then recast into a form similar to that of the existing models to allow for direct comparison between models.

This present model was then used to determine the effect of thermal diffusivity on specimen response. Under typical TMDSC operating conditions, it was found that as the sample thermal diffusivity decreased, a phase lag appeared between the applied temperature and the specimen response. It was also found that the amplitude of the sample temperature oscillation decreased as the sample thermal diffusivity decreased.

It was found that by incorporating specimen thermal diffusivity rather then only heat capacity the phase lag between the applied temperature oscillation and specimen response could be predicted. This phase lag was found to be dependent on thermal diffusivity rather than on c_p'', a poorly described and thermodynamically undefined parameter. Based upon this finding, the cyclic or modulated response can be expressed in terms of parameters associated with an effective thermal diffusivity of the sample. This definition has the advantage of being more consistent and associated to material properties that can be properly analyzed with in-phase and out-of-phase complex descriptions.

* * *

The authors express their appreciation to TA Instruments for continuous support to the Polymeric Composites Laboratory at the University of Washington. Support for this work was also provided by The Boeing Company through the Boeing-Steiner professorship.

Nomenclature

Roman letters

A	modulation amplitude/K
M_i'	magnitude of the in-phase component of the specimen temperature/K
M_i''	magnitude of the out-phase component of the specimen temperature/K
M_i^*	magnitude of the specimen temperature response/K
$A_{n,p}$	constant which was made τ dependent to solve the initial condition of the governing equation/–
L	specimen height/m
R	specimen radius/m
S	unitless source term that arises in the governing equation as a result of the change of variable/–
T	temperature/K
T_b	block (furnace) temperature/K
X	radial part of the product solution postulated for solving the governing equation/–
Z	axial part of the product solution postulated for solving the governing equation/
b	linear heating rate/K s^{-1}
c_p	specific heat capacity as define thermodynamically/J kg^{-1} K^{-1}
c_p'	in-phase component of the specific heat capacity/J kg^{-1} K^{-1}
c_p''	out-of-phase component of the specific heat capacity/J kg^{-1} K^{-1}
k	thermal conductivity/W m^{-1} K^{-1}
p	period of modulation/s
r	radial coordinate/m
t	time/s
z	axial coordinate/m

Indices

i	specimen (either reference or sample)
n	index of the radial eigenvalues
o	initial
p	index of the axial eigenvalues
r	reference
s	sample

Greek letters

$\bar{\Delta T}$	underlying part of the temperature difference between the reference and the sample/K
$\tilde{\Delta T}$	cyclic part of the temperature difference between the reference and the sample/K

Λ' effective thermal diffusivity term that arises in the in-phase component of the specimen temperature/$m^2\ s^{-1}$
Λ'' effective thermal diffusivity term that arises in the out-of-phase component of the specimen temperature/$m^2\ s^{-1}$
Ω azimuthal angle coordinate/rad
α thermal diffusivity/$m^2\ s^{-1}$
ζ dimensionless axial position/–
θ dimensionless temperature/–
κ eigenvalues depending on the sample geometry/–
λ eigenvalue related to the radial position/–
μ eigenvalue related to the axial position/–
ρ density/kg m^{-3}
σ summation term that arises in the ramp term of the specimen temperature/–
τ dimensionless time/–
φ phase angle between the specimen response and the block temperature/rad
ψ phase angle between the cyclic part of the temperature difference and the block temperature/rad
ω pulsation of the oscillation/rad s^{-1}

References

1 S. R. Sauerbrunn, B. S. Crowe and M. Reading, Proc. of the 21st NATAS Conference, Atlanta, Georgia 1992, p. 137.
2 M. Reading, D. Elliott and V. Hill, Proc. of the 21st NATAS Conference, Atlanta, GA 1992, p. 145.
3 M. Reading, R. Wilson and H. M. Pollock, Proc. of the 23rd NATAS Conference, Jacksonville, FL 1994, p. 2.
4 J. C. Seferis, I. M. Salin, P. S. Gill and M. Reading, Proc. of the National Academy of Athens, 67 (1992) 311.
5 N. O. Birge and S. R. Nagel, Phys. Review Letters, 54 (1985) 2674.
6 P. F. Sullivan and G. Seidel, Phys. Review, 173 (1968) 679.
7 S. R. Aubuchon and P. S. Gill, J. Thermal Anal., 49 (1997) 1039.
8 J. E. K. Schawe, Thermochim. Acta, 260 (1995) 1.
9 J. E. K. Schawe, Thermochim. Acta, 271 (1996) 127.
10 I. Alig, Thermochim. Acta, 304/305 (1997) 35.
11 G. W. H. Höhne, Thermochim. Acta, 304/304 (1997) 121.
12 J. M. Prausnitz, R. N. Lichtenthaler and E. Gomes de Azevedo, Molecular Thermodynamics of Fluid-phase Equilibria, PTR Prentice Hall, Englewood Cliffs, NJ 1986.
13 J. E. K. Schawe and G. W. H. Höhne, Thermochim. Acta, 287 (1996) 213.
14 S. H. Dillman and J. C. Seferis, J. Macromol. Sci., A26 (1989) 227.
15 J. C. Seferis and R. J. Samuels, Polymer Eng. and Science, 19 (1979) 975.
16 A. Boller, Y. Jin and B. Wunderlich, J. Thermal Anal., 42 (1994) 307.
17 J. A. Foreman, S. M. Marcus and R. L. Blaine, Proc. of the 52nd Annual Technical Conference ANTEC 94, San Francisco, CA 1994, p. 2156.
18 A. A. Lacey, C. Nikopoulos and M. Reading, J. Thermal Anal, 50 (1997) 279.

19 R. Melling, F. W. Wilburn and R. M. McIntosh, Anal., Chem., 41 (1969) 1275.
20 B. Schenker and F. Stäger, Thermochim. Acta, 304/305 (1997) 219.
21 F. B. Hildebrand, Advanced Calculus for Applications, Prentice-Hall, Englewood Cliffs, NJ 1976.
22 M. Abromowitz and I. A. Stegun, Eds., Handbook of Mathematical Functions with Formulas, Graphs, and Mathematical Tables, U. S. Government Printing Office, Washington, D. C. 1964.
23 F. P. Incropera and D. P. de Witt, Fundamentals of Heat and Mass Transfer, Wiley and Sons, New York 1990.
24 J. Brandrup and E. H. Immergut, Eds., Polymer Handbook, J. Wiley and Sons, New York 1989.
25 Commissions Romandes de Mathématique, de Physique et de Chimie, Formulaires et Tables, Editions du Tricorne, Geneva 1985.
26 Y. S. Touloukian, R. W. Powell, C. Y. Ho and M. C. Nicolaou, in Thermophysical Properties of Matter, Vol. 10, IFI/Plenum, New York 1973.